Chapter 2

Background theory: Atoms and light

"The most beautiful thing we can experience is the mysterious. It is the source of all true art and science." Albert Einstein

2.1 Optical forces

In order to understand the origin of light-induced atomic forces and their applications in laser cooling and trapping it is instructive to consider an atom oscillating in an electric field. When an atom is subjected to a laser field, the electric field, $\mathbf{E}$, induces a dipole moment, $\mathbf{p}$, in the atom as the protons and surrounding electrons are pulled in opposite directions. The dipole moment is proportional to the applied field, $|\mathbf{p}| = \alpha|\mathbf{E}|$, where the complex polarisability, α, is a function of the laser light's angular frequency ω_{L}.

The interaction potential, equivalent to the AC-stark shift, is defined as:

$$U_{\mathrm{Dip}} = -\frac{1}{2}\langle \mathbf{p}.\mathbf{E} \rangle = -\frac{1}{2\epsilon_0 c}\mathrm{Re}(\alpha) I(\mathbf{r}), \tag{2.1}$$

where the angular brackets indicate a time average, $I(\mathbf{r}) = \epsilon_0 c|\mathbf{E}|^2/2$ is the laser intensity, and the real part of the polarisability describes the in-phase component of the dipole oscillation. The factor of a half in front of eqn. (2.1)

is due to the dipole being induced rather than permanent. A second factor of a half occurs when the time average is made.

Absorption results from the out-of-phase component of the oscillation (imaginary part of α). For a two-level atomic system, cycles of absorption followed by spontaneous emission occur. Due to the fact that the above process depends explicitly on spontaneous emission, the absorption saturates for large laser intensities. There is no intensity limit on the dipole potential however. The scattering rate is defined as the power absorbed by the oscillator (from the driving field) divided by the energy of a photon $\hbar\omega_{\mathrm{L}}$:

$$\Gamma_{\mathrm{sc}}(\mathbf{r}) = \frac{\langle \dot{\mathbf{p}}.\mathbf{E} \rangle}{\hbar\omega_{\mathrm{L}}} = \frac{1}{\hbar\epsilon_0 c}\mathrm{Im}(\alpha)I(\mathbf{r}). \tag{2.2}$$

2.1.1 Two-level model

For a two-level atomic system, away from resonance and with negligible excited state saturation, the dipole potential and scattering rate can be derived semiclassically. To perform such a calculation the polarisability is obtained by using Lorentz's model of an electron bound to an atom with an oscillation frequency equal to the optical transition angular frequency ω_0. Damping is also introduced; classically this occurs due to the dipole radiation of the oscillating electron, however a more accurate model uses the spontaneous decay rate, Γ, of the excited state. If the ground state is stable, the excited state has a natural line width equal to Γ. The natural line width has a Lorentzian profile as the Fourier transform of an exponential decay is a Lorentzian. The two-level model expressions calculated by Grimm *et al.* (eqns. (10) and (11) in ref. [87]) are quoted here:

$$U_{\mathrm{Dip}}(\mathbf{r}) = -\frac{3\pi c^2\Gamma}{2{\omega_0}^3}\left(\frac{1}{\omega_0 - \omega_{\mathrm{L}}} + \frac{1}{\omega_0 + \omega_{\mathrm{L}}}\right) I(\mathbf{r}), \tag{2.3}$$

$$\Gamma_{\mathrm{sc}}(\mathbf{r}) = \frac{3\pi c^2\Gamma^2}{2\hbar{\omega_0}^3}\left(\frac{\omega_{\mathrm{L}}}{\omega_0}\right)^3\left(\frac{1}{\omega_0 - \omega_{\mathrm{L}}} + \frac{1}{\omega_0 + \omega_{\mathrm{L}}}\right)^2 I(\mathbf{r}). \tag{2.4}$$

The model does not take into account the excited state saturation and the multi-level structure of the atom. However, the above results are useful to understand

the scalings and the effect of the sign of laser detuning, which is defined as:

$$\Delta = \omega_{\mathrm{L}} - \omega_0. \tag{2.5}$$

Figure 2.1 shows pictorially the relationship between the frequencies and detuning. If the laser has a frequency less than the transition frequency ($\Delta < 0$) one calls this a *red-detuned* laser and the opposite case is called a *blue-detuned* laser.

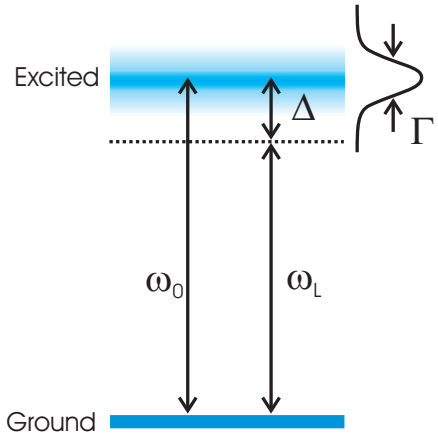

Figure 2.1: The two-level model showing the atomic transition angular frequency ω_0, the laser light's angular frequency ω_{L}, the detuning Δ and the natural line width of the excited state Γ.

For small detunings ($\Delta \ll \omega_0$ and $\omega_{\mathrm{L}}/\omega_0 \approx 1$), the *rotating wave approximation* (RWA) can be made and the $1/(\omega_0 + \omega_{\mathrm{L}})$ terms in eqns. (2.3) and (2.4) are ignored. This assumes that the term oscillates twice as fast as the driving frequency, and therefore time averages to zero. Under such an assumption the scalings of the dipole potential and scattering rate are:

$$U_{\mathrm{Dip}} \propto \frac{I(\mathbf{r})}{\Delta}, \quad \text{and} \quad \Gamma_{\mathrm{sc}} \propto \frac{I(\mathbf{r})}{\Delta^2}. \tag{2.6}$$

The consequence of such scalings will be explored further in Section 2.3. When the laser frequency is much lower than the atomic transition frequency, the static polarisability limit is reached. Such a limit is often referred to as the *quasi-electrostatic* (QUEST) regime. For alkali metal atoms this can be approximated by setting $\omega_{\mathrm{L}} \to 0$ in eqns. (2.3) and (2.4):

$$U_{\mathrm{Dip}}(\mathbf{r}) = -\frac{3\pi c^2}{{\omega_0}^3}\frac{\Gamma}{\omega_0} I(\mathbf{r}), \tag{2.7}$$

$$\Gamma_{\mathrm{sc}}(\mathbf{r}) = \frac{3\pi c^2 \Gamma^2}{\hbar {\omega_0}^3} \left(\frac{\omega_{\mathrm{L}}}{\omega_0}\right)^3 \left(\frac{\Gamma}{\omega_0}\right)^2 I(\mathbf{r}). \tag{2.8}$$

2.2 Laser cooling and the scattering force

In *Doppler cooling*, the scattering force is utilised in a way that makes it velocity dependent, resulting in a friction-like force which can be harnessed to cool atoms. The physical processes involved in laser cooling are described in detail in numerous sources, see for example refs. [2, 123] for a comprehensive description. A simplified account designed for teaching laser cooling to Physics A-level[1] students can be found in ref. [124]. A very brief sketch of the technique is presented below, before describing how it is applied to the specific case of cooling ^{85}Rb atoms.

The technique originates from the recoil kick an atom experiences when it absorbs a photon from a laser beam. The excited atom later decays via spontaneous emission and receives a second momentum kick. As the photon's spontaneous emission can occur in any direction, over many absorption-spontaneous emission cycles the second momentum kick averages to zero. Thus on average, for each cycle the atom receives a momentum kick of $\hbar\mathbf{k}$, where $\mathbf{k}$ is the laser wavevector, see Figure 2.2. The scattering rate is maximised on resonance ($\Delta = 0$), however the natural line width of the excited state means scattering can still occur off-resonance.

In order to take into account the saturation of the excited state population and to work close to resonance, the *Optical Bloch equations* are used (see, for example, ref. [123] or [125]). The scattering rate is given by:

$$\Gamma_{\mathrm{sc}}(\mathbf{r}) = \frac{\Gamma}{2} \frac{I(\mathbf{r})/I_{\mathrm{sat}}}{1 + I(\mathbf{r})/I_{\mathrm{sat}} + 4(\Delta)^2/\Gamma^2}. \tag{2.9}$$

The saturation intensity is given by:

$$I_{\mathrm{sat}} = \frac{2\pi^2 \hbar \Gamma c}{3{\lambda_{\mathrm{C}}}^3}. \tag{2.10}$$

[1] A *Further education* course in England and Wales taken by students 16–18 years old.

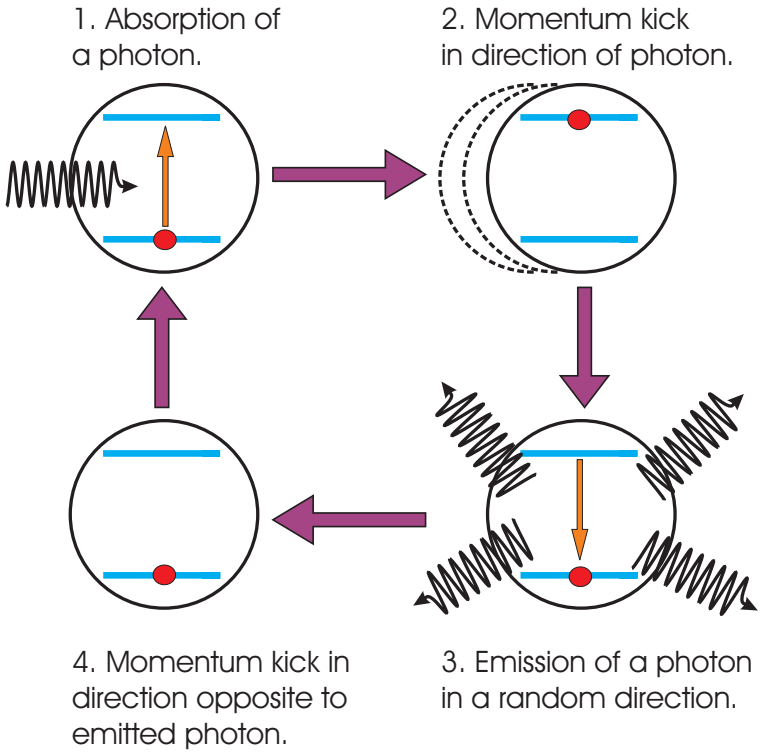

Figure 2.2: A simplified picture showing the absorption-spontaneous emission cycle that results in giving an atom a momentum kick.

For a Rb atom on the D2 line ($\lambda_C = 780$ nm, subscript C used to denote the cooling transition), and with a natural line width of $2\pi \times 5.9$ MHz [126], the saturation intensity is $I_{sat} = 1.6$ mW/cm^2.

A moving atom with velocity $\mathbf{v}$ will see the laser frequency Doppler shifted. This can easily be incorporated in eqn. (2.9) by making the replacement: $\Delta \rightarrow \Delta + \mathbf{k}.\mathbf{v}$. The scattering force is obtained by multiplying the scattering rate by the photon momentum $\hbar\mathbf{k}$. In the 1D case of two counter-propagating laser beams the scattering force is the resultant of the two beams, $F_{tot} = F_+ + F_-$, where the individual beam forces are:

$$F_\pm = \pm\frac{\hbar k\Gamma}{2}\frac{I/I_{sat}}{1 + 2I/I_{sat} + 4(\Delta \mp kv)^2/\Gamma^2}, \tag{2.11}$$

The extra factor of two in the denominator accounts for the contribution of the two beams towards the saturation of an atom. The forces of the individual beams, F_+ and F_-, and the total force, F_{tot}, are plotted in Figure 2.3. In the

regime $|kv/\Gamma| < 1$ the force can be approximated by:

$$F_{\rm tot} \simeq \frac{8\hbar k^2 \Delta}{\Gamma} \frac{I/I_{\rm sat}}{\left(1 + 2I/I_{\rm sat} + 4(\Delta/\Gamma)^2\right)^2} v = \beta\, v. \tag{2.12}$$

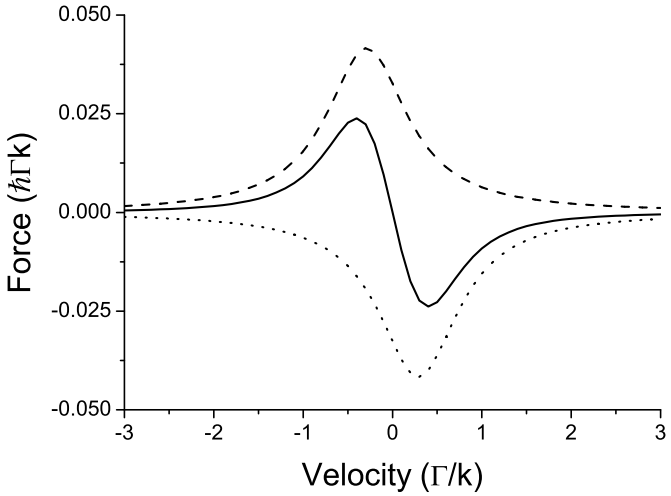

Figure 2.3: The combined force of two counter propagating red-detuned laser beams is plotted against velocity. The dashed line is F_+, the dotted line is F_-, and the solid line is the total force $F_{\rm tot}$. The parameters used to produce the plot were $I/I_{\rm sat} = 0.1$ and $\Delta/\Gamma = -1/\sqrt{12}$.

For red-detuned laser beams ($\Delta < 0$), β is negative and the force is friction-like, therefore resulting in cooling as the atom's kinetic energy is dissipated. It can be shown by taking the derivative of eqn. (2.12) that the maximum friction for weak beams is achieved when $\Delta/\Gamma = -1/\sqrt{12}$. The extension from 1D to 3D involves the use of 3 pairs of counter-propagating laser beams. This is called *optical molasses* due to the 'sticky' environment that the atom now moves in. The minimum temperature that can be achieved by Doppler cooling is given by balancing the cooling rate ($-\beta v^2$) with the heating rate due to the random nature of spontaneous emission ($(\hbar k)^2 \Gamma_{\rm sc}/m$). This temperature is called the Doppler limit [123]:

$$\mathcal{T}_{\rm D} = \frac{\hbar\Gamma}{2k_{\rm B}}. \tag{2.13}$$

Which for alkali metals is typically a few hundred μK. Sub-Doppler cooling mechanisms exist that overcome the Doppler cooling limit and can create an atomic gas with low μK temperatures. The origin of such mechanisms is the

spatial variation in the AC-stark shift due to polarisation gradients, see ref. [127] for more details.

2.2.1 The Magneto-optical trap

Whilst Doppler cooling can reduce the temperature of an atomic gas, it does not spatially confine the gas. Even at very low temperatures the atoms will escape from the cooling region due to Brownian motion random-walks. Raab *et al.* in 1987 invented a solution that combines optical and magnetic fields to both cool and trap the atomic gas [64]. Their solution involved applying a magnetic field linear with position to lift the degeneracy of the m_F states. In addition they used counter-propagating laser beams with opposite circular polarisations to produce $\sigma^{\pm}$ transitions. This results in an atom moving away from resonance being *Zeeman shifted* into resonance with a beam that pushes it back to the centre, see Figure 2.4 (a). The simplest combination of circularly polarised light and anti-Helmholtz coils to produce a quadrupole magnetic field is shown in Figure 2.4 (b). The design can be adapted to suit specific applications, see for example the pyramid MOT in Chapter 8.

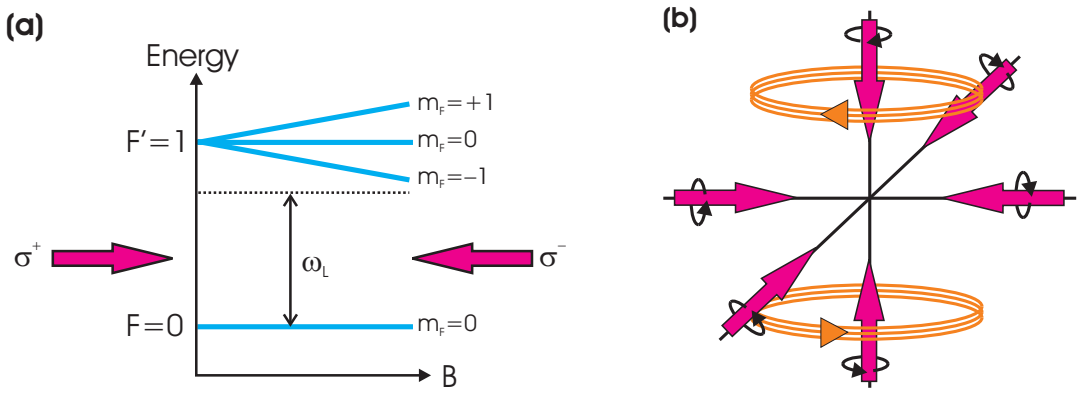

Figure 2.4: Plot (a): The principle of a magneto-optical trap is demonstrated for the $F = 0 \rightarrow F' = 1$ transition. An atom that has moved away from the trap centre is more likely to absorb a photon from the beam pushing it back. This results in a harmonic force. Plot (b): The simplest design for a 3D magneto-optical trap made from six circularly polarised laser beams. The anti-Helmholtz coils created a quadrupole magnetic field.

2.2.2 Implementing laser cooling in ^{85}Rb

In the above description it has been assumed that we are dealing with a two-level atom (with magnetic sub-levels). In reality atoms have a multi-level structure. It is possible though to find so called *closed transitions* that exploit the electric dipole selection rules to produce an approximation to a two-level system. For the case of ^{85}Rb, a closed transition occurs on the D2 line from $5^2S_{1/2}\,, F = 3$ state to the $5^2P_{3/2}\,, F' = 4$ state; where F is the total angular momentum of the atom and the prime indicates the excited state. This is illustrated in Figure 2.5.

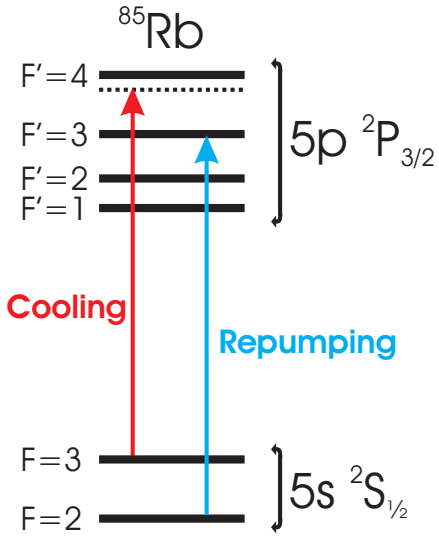

Figure 2.5: The energy level diagram for ^{85}Rb. The transition frequencies for the cooling and repumping lasers are also shown. This figure should be contrasted with the simpler two-level model in Figure 2.1. The level spacings are given in Appendix D.

Due to the selection rule $\Delta F = -1, 0, +1$ (see for example ref. [128]), the only decay route from the excited state is back to the original ground state, thus a closed cycle ensues. For cooling to occur, the laser frequency has to be red-detuned by a few line widths. Unfortunately there is a small probability that the transition from $5^2S_{1/2}\,, F = 3$ state to the $5^2P_{3/2}\,, F' = 3$ state will occur, as the laser is far blue-detuned from this frequency. Being in this excited state means that there is a probability that the atom will decay down to $5^2S_{1/2}, F = 2$ state, and thus be lost from the cycle. Therefore a second laser frequency is required to *repump* the lost atoms back into the cooling cycle. This laser operates on the $5^2S_{1/2}\,, F = 2$ state to the $5^2P_{3/2}\,, F' = 3$ state transition.

When laser cooling from a vapour, one typically uses a detuning of around -2Γ ($-2\pi \times 12$ MHz for Rb). The laser operates at a wavelength of $\lambda_C = 780$ nm which corresponds to a frequency of $\sim 10^{15}$ Hz. Care must be taken to know and accurately stabilise the laser frequency. This is discussed further in Chapter 8.

2.3 Laser trapping and the dipole force

The previous section outlined how the scattering force can be used to cool atoms with laser fields, we now turn to trapping them with light. The spatial variation of the intensity term in the dipole potential, eqn. (2.1), results in the conservative dipole force:

$$\mathbf{F}_{\text{Dip}} = -\nabla U_{\text{Dip}} = \frac{1}{2\epsilon_0 c}\text{Re}(\alpha)\nabla I(\mathbf{r}). \tag{2.14}$$

As can be seen from eqn. (2.6), a blue-detuned laser ($\Delta > 0$) will produce a positive AC-stark shift. Therefore the dipole force will cause atoms to be attracted to regions of low intensity. An atom will be attracted to red-detuned regions of high intensity. The scalings in eqn. (2.6) illustrate that a far red-detuned dipole trap with negligible scattering and sufficient trap depth requires a high intensity. For a CO_2 laser ($\lambda_T = 10.6$ μm, subscript T used to indicate the trapping laser's wavelength) this regime is readily achieved, as it is possible to buy bench-top lasers with powers of $\sim$ 100 W. Such a laser operates in the quasi-electrostatic regime, and eqn. (2.7) is an approximation of the dipole potential.

With knowledge of the polarisability and laser beam intensity profile, the force can be characterised via eqn. (2.14). In Chapter 3 laser beam profiles will be explained. The remainder of this chapter discusses the calculation of the polarisability in a more robust manner than the two-level approximation.

2.3.1 Polarisability

The real part of the polarisability has two parts: a scalar term, α_0, that corresponds to a dipole being induced parallel to the direction of the electric field and a tensor term, α_2, that corresponds to an induced dipole perpendicular to

the electric field. The scalar term shifts all hyperfine and magnetic sublevels equally. The tensor term mixes the hyperfine and magnetic sublevels through an operator Q, and therefore the degeneracy of the m_F states is lifted. The exception to this is for the ground state in alkali atoms ($J = 1/2$), where the lack of orbital angular momentum stops the spin-orbit coupling producing a perpendicular induced dipole moment and hence $\alpha_2 = 0$.

The light-shift is given by the eigenvalues of the matrix [129, 130]:

$$E = E_{\text{hfs}} - \frac{1}{2\epsilon_0 c}(\alpha_0 \mathbb{I} + \alpha_2 Q) I(\mathbf{r}), \tag{2.15}$$

where $\mathbb{I}$ is the identity matrix. The non–zero and diagonal matrix elements of the hyperfine interaction can be written in the $|F\, m_F\rangle$ basis as [131]:

$$\langle F\, m_F | E_{\text{hfs}} | F\, m_F \rangle = -\frac{\hbar}{2} A_{\text{hfs}}\, K + \hbar\, B_{\text{hfs}} \frac{\frac{3}{2}K(K+1) - 2I_{\text{n}}(I_{\text{n}}+1)J(J+1)}{2I_{\text{n}}(2I_{\text{n}}-1)\, 2J(2J-1)}\ , \tag{2.16}$$

where I_{n} is the nuclear spin quantum number, J is the total electronic angular momentum quantum number and K is defined as:

$$K = F(F+1) - I_{\text{n}}(I_{\text{n}}+1) - J(J+1)\ . \tag{2.17}$$

For the $5P_{3/2}$ states of ^{85}Rb, the hyperfine structure constants are $A_{\text{hfs}} = 2\pi \times 25.009$ MHz and $B_{\text{hfs}} = 2\pi \times 25.88$ MHz [132].

The matrix Q has components $\langle F m_{\text{F}} | Q_\mu | F' m'_{\text{F}} \rangle$ where:

$$Q_\mu = \frac{3\hat{J}_\mu^2 - J(J+1)}{J(2J-1)}. \tag{2.18}$$

The operator $\hat{J}_\mu$ is the electronic angular momentum operator in the direction of the laser field. When the electric field is aligned along the quantisation axis,

the non-zero elements in the Q-matrix in the $|F\, m_F\rangle$ basis are given by [133]:

$$\begin{aligned}\langle F\, m_F|Q|F'\, m_F\rangle = &\left[\frac{(J+1)(2J+1)(2J+3)}{J(2J-1)}\right]^{1/2} \\ &\times(-1)^{I_\mathrm{n}+J+F-F'-m_F}\sqrt{2(F+1)(2F'+1)} \\ &\times\begin{pmatrix} F & 2 & F' \\ m_F & 0 & -m_F \end{pmatrix}\begin{Bmatrix} F & 2 & F' \\ J & I & J \end{Bmatrix}.\end{aligned} \tag{2.19}$$

The object contained within the semi-circular brackets is a (3-j) symbol and the curly brackets contained a (6-j) symbol, see ref. [134]. It is interesting to note that the $|m_F|$ states are degenerate, a consequence of using a linearly polarised field. The general form of the Q-matrix for ^{85}Rb ($I_\mathrm{n} = 5/2$) is shown in Figure 2.6. When $m_F = \pm F_\mathrm{max}$ the problem is simplified as the two 1×1 matrices contain the value 1, thus $\alpha_\mathrm{max} = \alpha_0 + \alpha_2$.

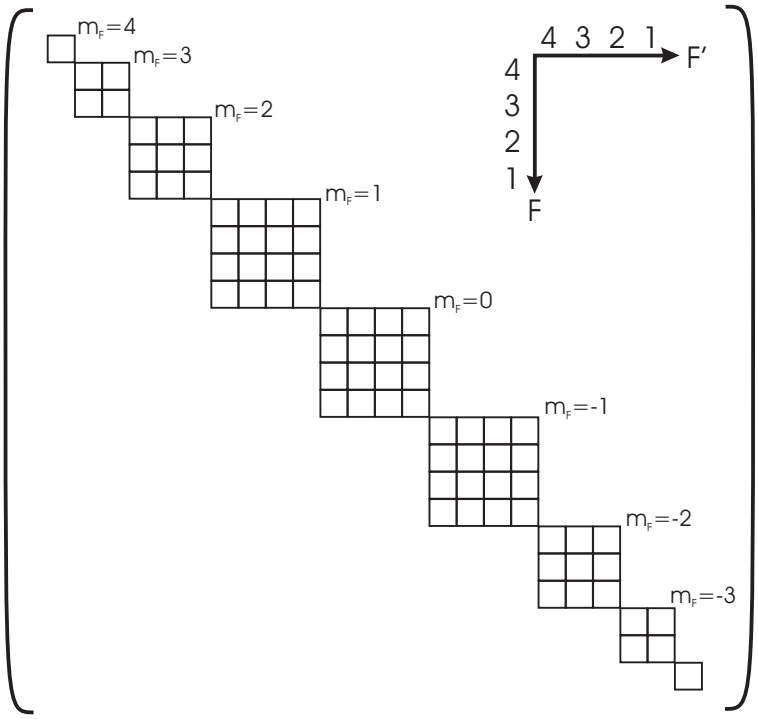

Figure 2.6: The general form of the Q-matrix for an atomic state $J = 3/2$, $I_\mathrm{n} = 5/2$. The non-zero matrix elements occur along the diagonal of the matrix.

The ground state shift

In most instances, knowledge of the ground state shift is sufficient to understand dipole trap dynamics. There is a vast simplification for the ground state shift; as already mentioned, the tensor polarisability is zero. Therefore, with knowledge of α_0, the dipole force is known through eqn. (2.14). Various groups have theoretically calculated and experimentally measured polarisabilities in Rb, see for example refs. [120, 135, 136, 137, 138, 139, 140]. Since for this thesis the light shifts of ^{85}Rb at only two wavelengths are needed (Nd:YAG $\lambda_T = 1.064$ μm and CO_2 $\lambda_T = 10.60$ μm), the relevant polarisabilities are quoted in Table 2.1 for two recent calculations. Griffin *et al.*'s calculations are non-relativistic and slightly overestimate the values Safronova *et al.* obtain in their relativistic calculations.

Polarisability	λ_T (μm)	Griffin *et al.* [120]	Safronova *et al.* [137, 140]
$\alpha_0[5s]$	1.064	722	693.5(9)
$\alpha_0[5p]$	1.064	-1162	–
$\alpha_2[5p]$	1.064	566	–
$\alpha_0[5s]$	10.60	335	318.6(6)
$\alpha_0[5p]$	10.60	872	–
$\alpha_2[5p]$	10.60	-155	–

Table 2.1: The scalar and tensor polarisabilities for Rb atoms. The two wavelengths quoted correspond to that of a Nd:YAG and CO_2 laser. To convert the values into SI units they must be multiplied by $4\pi\epsilon_0 {a_0}^3$, where a_0 is the Bohr radius (0.529 Å).

The differences between ground state polarisabilities for the two-level model from Section 2.1.1 and the more accurate multi-level calculations of Safronova *et al.* [137, 140] are tabulated in Table 2.2. For far-detuned lasers, the rotating wave approximation significantly underestimates the polarisability. The static limit for the CO_2 wavelength is within 1% of the two-level value. However, all values based upon the two-level model have a $\sim 7\%$ underestimate of the polarisability calculated by including multi-level structure. Therefore, the values of Safronova *et al.* will be used throughout this thesis for calculating dipole traps.

State	λ_T (μm)	2-level model	RWA	Static limit	Polarisability [137, 140]
$\alpha_0[5s]$	1.064	642.5	556.8	–	693.5
$\alpha_0[5s]$	10.60	298.9	160.4	297.2	318.6

Table 2.2: A comparison of the ground state polarisability calculated using: the two level model (eqn. (2.3)); the rotating wave approximation applied to eqn. (2.3); the static limit (eqn. (2.7)); Safronova *et al.* calculated polarisability [137, 140]. To convert the values into SI units they must be multiplied by $4\pi\epsilon_0 {a_0}^3$, where a_0 is the Bohr radius (0.529 Å).

The excited state and differential-shifts

As can be seen in Table 2.1, the ground and excited states have different polarisabilities, resulting in a *differential light-shift*. This has consequences if in addition to a laser trapping the atoms, there is also a separate Doppler cooling laser present. A common occurrence in far-detuned dipole trap experiments is to have the trap laser switched on throughout the cooling and MOT loading process, then, when the cooling beams are switched off, a fraction of the atoms gets loaded into the trap. A differential light shift means that the cooling laser's detuning becomes dependent on the intensity of the trapping laser – generally an unwanted effect.

The sign of the polarisability of the excited state changes between the Nd:YAG and CO_2 laser wavelengths. The Nd:YAG laser light shifts the excited state upwards, whereas the CO_2 laser shifts the state downwards. The effect on detuning is illustrated in Figure 2.7. The Nd:YAG laser causes the red-detuned cooling laser to be further detuned. However, the CO_2 laser causes the detuning magnitude to decrease, and at some point the detuning will turn positive. For deep potential wells, this causes the focus region, where the intensity is greatest, to heat the atoms. This has been observed experimentally, see for example ref. [94]. Griffin *et al.* experimentally demonstrated that, using a combination of a Nd:YAG and CO_2 laser, the excited state shift can be engineered to be the same as the ground state shift, hence causing enhanced trap loading [120].

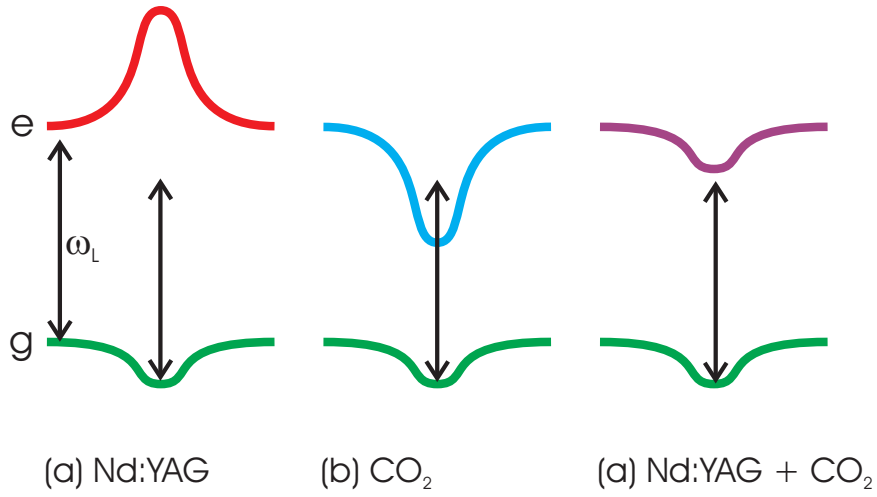

Figure 2.7: The differential light-shift for three combinations of trapping lasers are illustrated: (a) Nd:YAG laser only, the negative excited state polarisability shifts the level upwards causing the cooling laser to be further red-detuned; (b) CO_2 laser only, the positive excited state polarisability shifts the level downwards causing the cooling laser to be blue-detuned for sufficient trapping laser intensities; (c) Nd:YAG and CO_2 lasers, when the powers have been chosen correctly the differential light-shift is canceled [120].

Chapter 2 summary

- The physical origin of the scattering and dipole forces was described.
- A two-level atomic model was presented that led to intensity and detuning scalings.
- The technique of laser cooling was described along with how it is implemented in ^{85}Rb.
- The scalar and tensor polarisability contributions to the the dipole force were discussed. The approach was compared with the simpler two-level approach.
- The differential light-shift and the problem this causes with dipole trap loading was explained. The concept of light-shift engineering was introduced.